Nanoscale

PAPER

View Article Online
View Journal



Cite this: DOI: 10.1039/c7nr06992h

# Nanomechanical clinical coagulation diagnostics and monitoring of therapies†

Francesco Padovani, James Duffy and Martin Hegner *

Clinical coagulation diagnostics often requires multiple tests. Coagulation times are a first indication of an abnormal coagulation process, such as a coagulation factor deficiency. To determine the specific deficient factor, additional immuno- and/or enzyme assays are necessary. Currently, every clinical laboratory has to normalize their assays (international normalized ratio, INR), and therefore, certain variability within the clinical analytics exists. We report a novel strategy for a quick, reliable and quantitative diagnosis of blood coagulation diseases (*e.g.* haemophilia) and for monitoring factor replacement and anticoagulant therapies (*e.g.* heparin treatment). We exploit nano-oscillations of microcantilevers for real-time measurements of the evolving blood plasma clot strength (viscosity). The sensors are oscillated at multiple high resonance mode numbers, in order to minimise the oscillation amplitude (a few nanometers), to provide direct internal control and to increase the quality factor. Along with the activated thromboplastin time (aPTT) and prothrombin time (PT) other parameters important for thrombosis diagnostics can be obtained, including the final clot strength and the fibrinolysis time. We demonstrate the dependence of the parameters on factor deficiencies and we diagnose a specific factor deficiency through an integrated and quantitative *in situ* immunoassay. This approach does not require continuous calibration since it delivers an absolute quantity (clot strength). The low sample volume required (a few μl) and the ability to measure different parameters within the same test (PT, aPTT and global coagulation assay) make the presented technique a versatile point-of-care device for clinical coagulation diagnostics.

Received 19th September 2017,
Accepted 23rd October 2017

DOI: 10.1039/c7nr06992h

rsc.li/nanoscale



## Introduction

Hemostasis is a physiological process that leads to sealing of a vasculature break. It must be well regulated, fast and localized. Coagulation is the result of a complex sequence of biochemical reactions, called the coagulation cascade (Fig. 1a). After the clot has been formed, coagulation must be stopped and, after healing, the clot has to be dissolved. From a clinical point of view, the coagulation cascade is divided into three pathways: intrinsic (contact activation), extrinsic and common. The final active product of the common pathway is the protein thrombin. Thrombin cleaves fibrinogen into fibrin that is further polymerized and crosslinked by factor XIII. Once the clot reaches healthy endothelial tissue, the anticoagulation cascade is triggered, coagulation is stopped and later the fibrin clot is dissolved. Any unregulated activity in this sequence of reactions would lead to a pathological disorder. Fast, accurate and reliable determination of multiple coagulation parameters is vital to a correct diagnosis of blood coagulation disorders. Two of the most common coagulation assays performed regularly in a hospital environment are the prothrombin time (PT, induced by an excess of tissue factor, extrinsic and common pathways) and the activated partial thromboplastin time (aPTT, induced by surface activation, intrinsic and common pathways). These two assays measure the time required for the onset of fibrinogen proteolysis that is followed by the formation of a fibrin network.[1] Clot formation is usually detected by increased impedance or turbidity. Any prolongation of one of these two times corresponds to a factor deficiency or inhibition to one (or more) of the corresponding pathway's proteins.[2] Both assays are extremely useful but have some drawbacks and always require further testing. First of all, they are not factor specific and they are sensitive only if the factor activity is lower than 50%. Secondly, they stop at the moment of "thrombin burst" and they do not assess the polymerization rate nor the factor XIII crosslinking activity and subsequent fibrinolysis. Thirdly, the initial blood plasma viscosity, the clot strength and its ability to hold blood flow pressure are not measured. Lastly, both assays do not evaluate bleeding or thrombosis risk and do not monitor acute bleeding.[2] These drawbacks demand for the development of novel strategies that can improve the clinical diagnosis process. These so-called global hemostasis assays have gained attention in recent years. Global hemostasis

*Centre for Research on Adaptive Nanostructures and Nanodevices (CRANN), School of Physics, Trinity College Dublin, Ireland. E-mail: martin.hegner@tcd.ie*

† Electronic supplementary information (ESI) available: Additional experimental details, methods and figures. See DOI: 10.1039/c7nr06992h

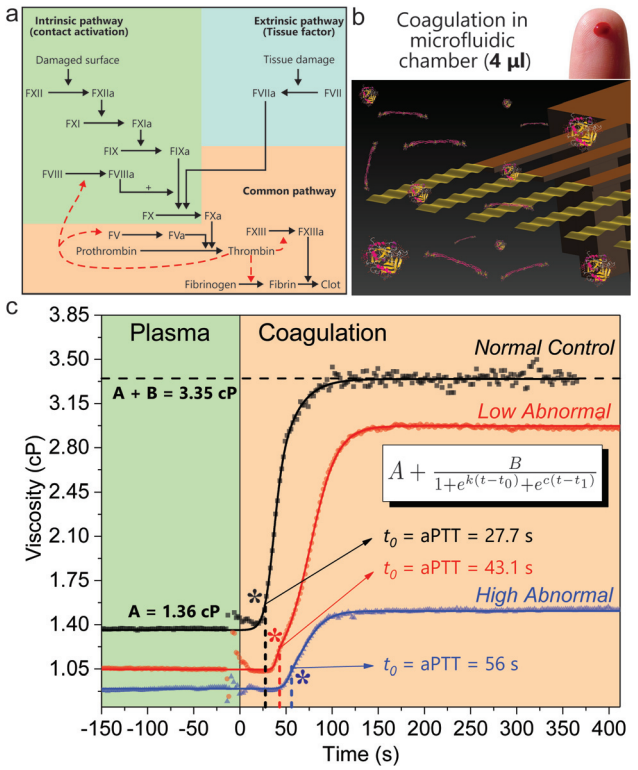


**Fig. 1** Determination of the coagulation parameters. (a) Coagulation cascade schematics. Highlighted in green are the factors of the intrinsic pathway, in light blue are the factors of the extrinsic pathway and in orange are the factors of the common pathway. (b) Representation of the suspended microresonators oscillating at high speeds (~300 kHz). (c) Viscosity changing over time during coagulation. The sensor array is first immersed in plasma (green area) and then at time 0 s the coagulation is triggered with aPTT reagents (orange area). Three different samples were tested: normal (black curve), low abnormal (red curve) and high abnormal (blue curve) control plasma. These samples have been used to calibrate the device. Each curve is the average of 4 measurements (error bars are too small to be visible). A specific mathematical model (modified logistic function, see equation I in the figure) is fitted to the viscosity data in order to extrapolate the coagulation parameters. Clinically relevant parameters are $A$ (plasma viscosity), $A + B$ (clot viscosity) and $t_0$ (aPTT or PT, coagulation times). Time $t_0$ (* symbol) corresponds to the transition between the first slow viscosity change stage and the second fastest viscosity change stage. For the other biological parameters, clinical relevance needs to be established. All the parameters are required for the accurate and reliable fitting process.

aims to measure the viscoelastic properties of the blood clot in order to assess the global clot strength once it is formed. Two of the most adopted global assays are thromboelastography (TEG)[3] and rotational thromboelastography (ROTEM).[4,5] The goal of these assays is to analyse in real time the process of clot formation,[6] clot stability,[7] and clot resolution (fibrinolysis).[8–10] Other global assays are thrombin generation (TG)[11] and overall hemostasis potential (OHP).[12] All of these assays suffer from a wide variation in results, they are not factor specific, and the output values are not absolute, but related to the particular technique employed. Furthermore, they usually require a large sample volume (300 µl to millilitres). Novel approaches that exploit micro- and nanotechnology have been developed in recent years, such as quartz crystal microbalance (QCM)[13,14] and surface plasmon resonance (SPR).[15] These strategies greatly reduce the amount of the sample needed. However, with QCM it is not possible to distinguish between protein adsorption and liquid viscoelasticity changes, reducing the potential to determine the overall clot strength. SPR on the other hand does not suffer from this drawback but the measured variables are not absolute and only the PT was previously measured.[16] We previously reported a novel strategy to measure aPTT exploiting microcantilever-based resonators.[17] Here we show the ability of this strategy to diagnose different blood coagulation disorders, using a smaller amount of the sample (a few microliters). We present a new mathematical model to extrapolate PT and aPTT along with global hemostasis parameters (blood plasma viscosity, clot formation, stability and dissolution) and factor specificity in one single assay. The measured global variable is the viscosity of human blood plasma changing during coagulation and clot dissolution. As the viscosity is measured in centipoise (1 cP = 1 mPa s), the presented assay has high potential for standardization. Our approach employs the evaluation of the nanomechanical response of suspended micro-resonators (immersed in fluid) whose oscillation frequency and quality factor are dependent on the density and the viscosity of the liquid surrounding the structure.[18] In recent years, micro-resonators have been successfully used as biosensors to detect biomarkers,[19,20] to monitor single microbial cell growth,[21] to characterize sperm motility,[22] to study the thermodynamics of biomolecule surface transformations[23,24] and to measure the viscosity of small sample volumes[25–27] (in the order of a few µl). However, measurements of biologically relevant liquids that contain proteins require special care. Proteins tend to stick and unspecifically adsorb onto solid surfaces and they might undergo conformational changes and subsequent loss of activity.[28] In our recent work,[17] we optimised the resonating micromechanical sensor surfaces exposed to human blood plasma to make them biocompatible and to minimise unspecific protein adsorption. We showed that tracking of multiple modes at high resonant frequencies (hundreds of kHz) increased the quality factor and minimised the total acoustic energy released in the surrounding fluid. The oscillation amplitude at high mode numbers is in fact in the order of a few nanometres (see the ESI of ref. 17). The tracking of multiple modes also provides an internal control, because tracking more than one peak allows for enhanced evaluation when the peaks shift synchronously.[29] Here we report the capability of the assay to measure specific factor deficiencies and their effects on clot strength. Furthermore, we monitor the coagulation development over time in different blood related disorders. The clot stability, clot dissolution (fibrinolysis) and the effects of anticoagulant drugs on the clot formation process are analysed as well. All these parameters will expand and improve clinical coagulation diagnostics and would enable the monitoring of therapies for coagulation disorders. The small size of the microfluidic

 

chamber (4 μl) allows for further miniaturisation and enables point-of-care testing.

## Experimental section

### Materials

The hetero-bifunctional compound (11-mercaptoundecyl)tetra (ethylene glycol) for a hydrophilic, neutral terminus (PEG) surface functionalization, 1,4-dioxane (99.8%), ethanolamine (≥98%), thrombin, human serum albumin (HSA), fibrinogen (from human plasma, lyophilized powder), and tissue plasminogen activator (tPA) were purchased from Sigma Aldrich, Ireland. Dithiobis(succinimidyl undecanoate) (DSU) was purchased from Dojindo Molecular Technologies, Japan. Pepsin/hydrochloric acid for the removal of proteins was purchased from VWR Ireland. Fibrinogen was reconstituted in 0.9% NaCl in 1 mM HEPES buffer (≥99.5%) at pH 6.8 at 10 mg $ml^{-1}$ and diluted down to the required concentration when needed. Thrombin was reconstituted in 0.1% HSA at 350 NIH[30] unit per ml and then diluted down to 70 NIH unit per ml prior to the experiment. Tissue plasminogen activator was reconstituted in nanopure water at 1 mg $ml^{-1}$ and diluted down to 350 ng $ml^{-1}$ when utilized. HemoSIL® human blood plasma normal control, high abnormal control, low abnormal control, low fibrinogen control, low heparin control, high heparin control, factor VIII and IX deficient plasma, aPTT kits, and PT reagents (RecombiPlasTin 2G) were all purchased from Brennan&Co, Ireland. Factor XIII deficient plasma was purchased from Quadratech Diagnostics, United Kingdom, and factor XIII concentrate (fibrogammin, CSL Behring) from Allphar Ltd, Ireland. Plasma controls were reconstituted in 1 ml of nanopure water, prior to the experiment. PT and aPTT kits were ready to use. Fibrogammin was reconstituted in water or 0.9% NaCl solution at 250 IU $ml^{-1}$ and diluted down to 2 IU $ml^{-1}$. One millilitre of the resulting solution was used to reconstitute FXIII deficient plasma or 2.5 mg of fibrinogen. Antibodies (GMA-012 anti-factor VIII and 13F42-F6 anti-factor IX) were purchased at a concentration of 6.7 μM (IgG1, 150 kDa, 1 mg $ml^{-1}$) from Abcam, United Kingdom.

### Experimental device

The experimental device has been described fully in our previous work (see ref. 17 and 31). Arrays of 8 cantilevers were clamped into a microfluidic chamber (volume 4 μl) where liquids were exchanged by automated syringe pumps and a micro-dispensing injection valve. The sensor oscillations are driven by a piezoelectric element placed underneath the array chip. The optical laser readout allows the tracking of the phase and amplitude spectra of the oscillating structures. Resonance frequencies and quality factors are evaluated from the spectra as explained in ref. 17. In these previous studies, we have optimized the surface chemistry of the sensors to minimize protein adsorption and we have tracked absolute viscosity and density changes occurring during human blood plasma coagulation in real time.

### Microarray chip preparation

Arrays of 8 microcantilevers (IBM Zurich Research Laboratory, Switzerland) with a length, width and thickness of 500 μm, 100 μm and 1 μm, respectively, were cleaned, coated and functionalized with two different functionalization procedures. For viscosity measurements without antibodies, we minimized protein adsorption with a PEG terminated monolayer using a recently reported protocol.[17] For the immobilization of antibodies onto gold surfaces, we used the *N*-hydroxysuccinimide (NHS) ester linker method.[32–34] First, the array was immersed in 1 mM dithiobis(1-succinimidyl undecanoate) (DSU) in 1,4-dioxane for 30 minutes. The chip was then thoroughly rinsed first with 1,4-dioxane, secondly with acetone and then with 20 mM HEPES buffer at pH 6.8. This step creates a NHS-terminated SAM that covalently binds to a primary amine group of the antibodies.[34] The microcantilevers were then functionalized selectively by immersing in 6.7 μM solutions of two different antibodies for 1 hour in individual micro-capillaries.[32] GMA-012 anti-factor VIII antibody solution contains 1% mannitol, 0.15 M NaCl and 10 mM sodium phosphate at pH 7.4, while 13F42-F6 anti-factor IX antibody contains 0.7% sodium phosphate, 0.03% EDTA and 0.58% sodium chloride at pH 6.6.

## Results and discussion

### Determination of coagulation parameters

Accurate and repeatable evaluation of coagulation times such as PT and aPTT is crucial in blood tests in clinical environments. To achieve these requirements, we exploited suspended microresonators that oscillate at high speeds (Fig. 1b). The damping (measured by the quality factor) and the speed (resonance frequency) of the oscillations are correlated with the viscosity and density of the liquid surrounding the structure.[17] When coagulation is triggered, the viscosity increases due to the formation of the fibrin network (see Fig. 1a). The coagulation assays PT and aPTT measure the time required for the onset of fibrinogen proteolysis associated with a sudden viscosity increase (fibrin polymer network). We propose a mathematical model that can describe the clot strength development over time. The equation that describes the model is the following:

$$\eta(t) = A + \frac{B}{1 + e^{k(t-t_0)} + e^{c(t-t_1)}} \quad (1)$$

where $\eta(t)$ is the change in the plasma viscosity during coagulation and $A$, $B$, $t_0$, $t_1$, $k$ and $c$ are fitting parameters. This model includes a baseline that corresponds to the plasma viscosity (parameter $A$, Fig. 1c), the final clot strength (given by $A + B$, Fig. 1c), two slopes that correspond to the initial and final coagulation rates (parameters $k$ and $c$, Fig. 1c) and two coagulation times (parameters $t_0$ and $t_1$). Note that eqn (1) represents a new and more powerful method than the one presented in our previous work.[17] Our previous method was based on a simple linear fit of the sudden viscosity change

occurring straight after reagent injection. Therefore, it relies on the assumption that the viscosity changes linearly over time. While the assumption proved to be acceptable, we believe that an improved description of the overall process was required. The newly presented mathematical model (eqn (1)) describes the whole coagulation process, from the initial plasma viscosity to the final clot strength. Furthermore, it does not extrapolate only the coagulation time, but also five other clinically relevant parameters ($A$, $B$, $k$, $c$ and $t_1$). Finally, it suffers from less uncertainty in the determination of the sudden viscosity change starting point. The viscosity change shows three different stages: (a) a slow start, (b) a sudden increase and (c) a clot strength change rate decreasing before reaching a stable viscosity value. While the previous model described only stage b, the new model contains a mathematical description for all these stages, increasing the accuracy in the determination of the coagulation times. In order to prove the validity of this model, we tested three different plasma samples that have been designed to have a specific PT or aPTT when tested with commercially available devices (see Table S1†) called normal control, low abnormal and high abnormal controls. When the model described above is fitted to the viscosity data, the parameter $t_0$ corresponds to the aPTT (see Fig. 1c) or PT (see Fig. S1†). Note that all the parameters extracted have a clinical relevance, but they are not measured in standard PT or aPTT tests. In particular, $A$ (plasma viscosity) could be directly correlated with hyperviscosity,[35] $A + B$ (clot strength) was found to be inversely proportional to the control abnormality (the higher the abnormality, the lower the clot strength), while for $k$, $c$ and $t_1$, a clinical connection to a disease state has to be established. All the parameters are fundamental for an accurate and adequate fitting process. As described in our previous work,[17] higher viscosity values correspond to lower quality factors. Lower quality factors increase the uncertainty in the fitting process, increasing the noise around both the resonance frequency and quality factor. For normal control plasma (the highest viscosity value), the signal-to-noise ratio is lower than all other abnormalities presented (see Fig. 1 and 3). The coagulation times extracted from the viscosity curves are within the expected range (see Table S1†). The test can be repeated up to three times using the same array of sensors after a pepsin/hydrochloric acid cleaning procedure (see Fig. S2†). Note that plasma proteins lose their activity over time (plasma can be considered stable for 4 hours after reconstitution), resulting in a lower initial plasma viscosity and lower final clot strength after a few hours (see Fig. S2†).

### Fibrinogen disorders

Two different hereditary categories of plasma fibrinogen defects exist: a quantitative fibrinogen deficiency called afibrinogenemia or hypofibrinogenemia and a qualitative fibrinogen deficiency called dysfibrinogenemia or hypodysfibrinogenemia. Bleeding severity can range from mild to severe.[2] Both deficiencies may prolong the PT and aPTT, but only if the fibrinogen concentration is below 1 mg ml$^{-1}$ (healthy physiological fibrinogen concentration range is 1.5–4 mg ml$^{-1}$). Dysfibrinogenemia is usually asymptomatic, but it may be associated with thrombosis.[36] Thrombotic events have also been reported in patients with afibrinogenemia.[37,38] To evaluate the effects of fibrinogen on the final clot strength, we first tested different fibrinogen concentrations mixed with a constant concentration of thrombin solutions (70 NIH[30] units per ml). Fig. 2 shows the final clot viscosity of the mixture at 37 °C in the fibrinogen concentration range 0.5–3.5 mg ml$^{-1}$. Note that the viscosity of water at 37 °C is about 0.7 cP. As expected, higher fibrinogen concentrations increase the final clot strength. However, the fibrin network formed is not cross-linked due to the absence of factor XIII and even with high fibrinogen concentrations the clot strength was considerably lower than a normal plasma clot. Next, we measured how the clot strength develops over time when an aPTT reagent (see Materials and methods) is added to two different plasma samples: a low fibrinogen plasma control (fibrinogen concentration below the physiological range) and a low abnormal plasma control with the addition of 2.5 mg ml$^{-1}$ of fibrinogen (Fig. 3).

In the first case, the aPTT is prolonged and the final clot strength was significantly low. In the second case, the aPTT remains comparable to a low abnormal plasma control, but the final clot strength was in the same range (~3 cP) of a normal plasma control. This result indicates that there are still other elements that cause the prolonged aPTT (low abnormal plasma has many factor concentrations in the low abnormal range), even though the normal concentration of clottable fibrinogen has been restored. A low clot strength could indicate a fibrinogen defect. To diagnose it, the clot strength should shift to the normal range when fibrinogen is added to the sample prior to coagulation.

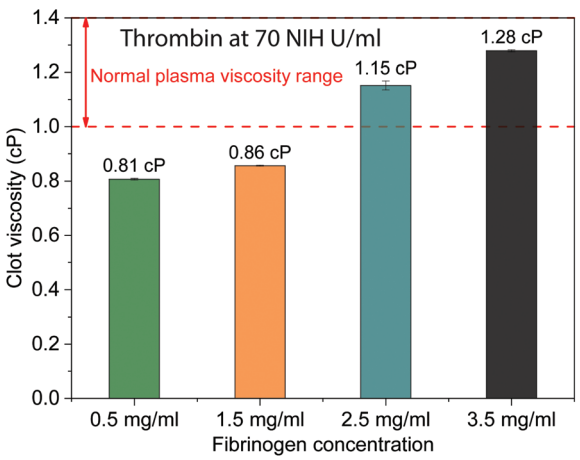


**Fig. 2** Thrombin and fibrinogen final clot viscosity at different fibrinogen concentrations. Physiological concentration of fibrinogen in blood plasma is 2–4 mg ml$^{-1}$. Thrombin was kept constant at a concentration of 70 NIH units per ml. Viscosity is a measure of the clot strength and it is directly proportional to fibrinogen concentration. Uncertainty in the measure is in the range 0.02–0.08 cP.

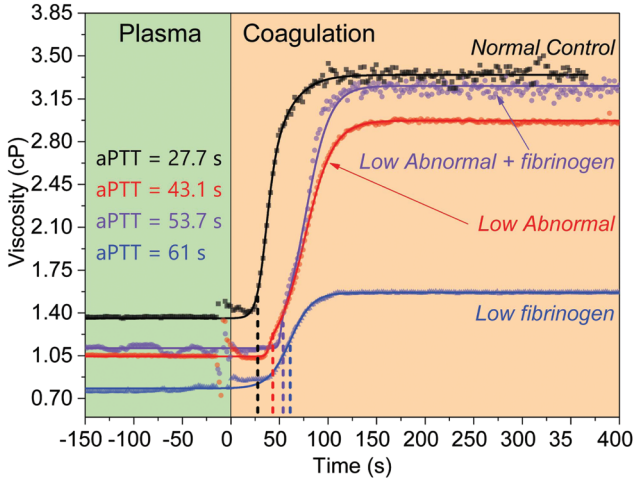


**Fig. 3** Fibrinogen concentration effects on the development of the clot strength over time during an activated partial thromboplastin time (aPTT) test. The microresonators are first immersed in plasma (green area) and then at time 0 s the coagulation is triggered with aPTT reagents (contact activation, orange area). The black curve shows the viscosity change for a normal control plasma, the red one for a low abnormal plasma, the blue one for a low fibrinogen concentration plasma, and the violet plot shows a low abnormal plasma with the addition of 2.5 mg $ml^{-1}$ of fibrinogen solution. Each curve is an average of 4 measurements (error bars are too small to be visible). Note that a low abnormal plasma is human blood plasma that has been modified to simulate an abnormality with a specific prolonged aPTT (see HemosIL datasheet, Werfen and ESI†). Human blood plasma at a low fibrinogen concentration (blue curve) shows a prolonged aPTT and a low final clot strength (low viscosity). Low abnormal plasma has a low fibrinogen concentration (along with other abnormalities). Physiological fibrinogen concentration is restored by adding 2.5 mg $ml^{-1}$ of fibrinogen solution the final clot strength is in the normal range, while the aPTT is still prolonged.

### Hemophilia and factor XIII deficiency

Hemophilia A (factor VIII deficiency) and B (factor IX deficiency) are the most common bleeding disorders affecting 1 in 5000 to 10 000 males and 1 in 30 000 males, respectively. It is an X chromosome linked disorder that essentially affects males. The bleeding severity ranges from mild (6–30% factor activity) to moderate (1–5% factor activity) to severe (<1% factor activity).[39,40] Bleeding is most common in the hinge joints and it can lead to structural deterioration, acute and chronic pain, and muscle atrophy with disability. Factor XIII is fundamental for the cross-linking of fibrin networks and stabilizing blood clots.[41] Factor XIII deficiency can lead to delayed bleeding (24 to 36 hours) after surgery or trauma. Coagulation assays like PT and aPTT do not measure cross-linking, therefore they appear to be normal in factor XIII deficient plasma. Diagnosis is performed usually with a specific immunoassay for factor XIII. For both haemophilia and factor XIII deficiency, treatment is carried out with frequent replacement of factor products. The first recombinant factor XIII has been recently approved by the US Food and Drug Administration[42] and a quick global assay would be beneficial. In severe or moderate haemophilia, the aPTT is prolonged, while the PT is normal. In mild haemophilia, the aPTT might be normal. To diagnose a specific factor deficiency, the first approach is normally a mixing test. The aPTT in fact should be restored to normal values when the factor deficient plasma is mixed with 50% of normal control plasma. Further testings (*e.g.* immunoassay) are then required to determine the specific factor deficiency and its activity. Notably, the final clot strength for the three levels of haemophilia was always significantly lower (~1.5 cP) than a normal plasma clot strength (~3.2 cP) (Fig. 4a). The aPTT was almost entirely restored with 30% factor activity (by addition of 30% normal control plasma). However, the clot strength was still low. The specific factor deficiency and its activity were addressed by functionalizing the surfaces of the resonators with different antibodies. Dithiobis(1-succinimidyl-undecanoate) (DSU) was used as a linker between the gold surfaces of the sensors and the antibodies (see Materials and methods). To include a passive control surface, some DSU functionalized surfaces that were not functionalized with antibodies were exposed to ethanolamine. Ethanolamine passivates and quenches the DSU surface.[32] Three sensors were functionalized with factor VIII antibodies (anti-FVIII), three with factor IX antibodies (anti-FIX), and two with quenched DSU (qDSU). An aPTT test with factor IX deficient plasma was then performed. The mass adsorbed onto the sensors was calculated according to ref. 29. During the first exposure to plasma, anti-FVIII surfaces adsorbed a significantly higher mass compared to both anti-FIX and qDSU surfaces (Fig. 4b). The difference between anti-FVIII and anti-FIX provides the specific factor VIII adsorption from the plasma sample. Note that factor VIII circulates in plasma bound to the Von-Willebrand factor (vWF)2. After triggering the coagulation, the signal-to-noise ratio (SNR) of the anti-FVIII sensors during the stable clot phase is significantly lower (higher SNR-1) than anti-FIX and qDSU sensors. This lower SNR indicates a continuous mass adsorption–desorption caused by motion-release of the high molecular weight Von-Willebrand factor. The specific factor IX deficiency was therefore directly confirmed through a differential measurement (FVIII–FIX). Note that the aPTT and the final clot strength were measured within the same experiment (Fig. 4a). The final clot strength was in a high abnormal range and the aPTT was significantly prolonged. A second possible approach to diagnose a factor deficiency is to add a specific factor to a deficient plasma and test whether the coagulation times and the final clot strength are restored or not. We tested factor XIII deficient plasma and we proved that despite a normal PT the final clot strength is significantly lower than normal control plasma (Fig. 4c). After the addition of 2 IU $ml^{-1}$ of factor XIII (as per clinical guidelines), the final clot viscosity was restored back to the normal range. For the effects of factor XIII added to thrombin and fibrinogen solutions, see Fig. S3.†

### Thrombosis diagnostics and heparin therapy

The duration, location and amount of clot formation at the site of injury need to be well regulated to prevent the uncontrolled growth of a hemostatic plug. Any disorder in these

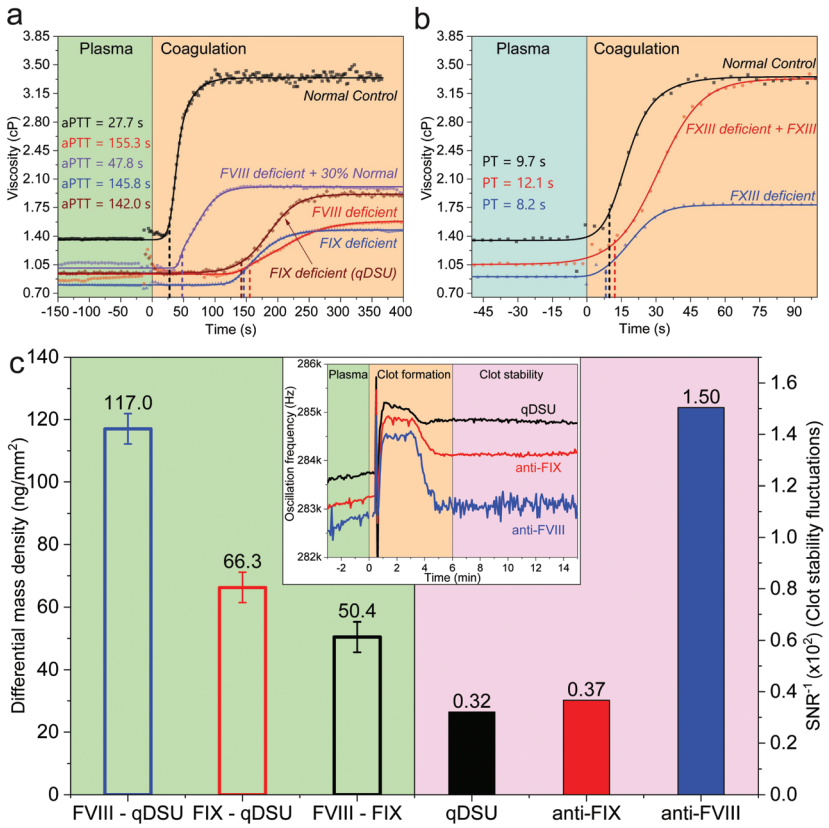


**Fig. 4** Specific factor deficiency diagnosis. (a) Clot strength development during an activated partial thromboplastin time (aPTT) test for different factor deficiencies and surface coverage for different self-assembled monolayers (SAMs). The array of sensors is first immersed in human blood plasma (green area) and then at time 0 s the coagulation is triggered with the specific reagents (orange area). Both factor VIII (haemophilia A, red curve) and factor IX (haemophilia B, blue curve) deficient plasma showed a prolonged aPTT and a low final clot strength (see parameter $A + B$ in Fig. 1). When 30% of normal plasma is mixed with factor VIII deficient plasma (mild haemophilia A, violet curve), both the aPTT and the final clot strength are more similar to a normal range, but they are still in the low abnormal range. The final clot strength of quenched DSU surfaces (qDSU, brown curve) is higher than that of PEG surfaces (light blue and red curves) because qDSU has slightly lower performances in terms of protein adsorption compared with PEG, therefore it shows higher unspecific mass adsorption. The unspecific mass adsorption leads to a minimal distortion in the viscosity measurement. (b) Clot strength development plot during a prothrombin time (PT) test for a factor XIII deficient plasma (blue curve), factor XIII deficient plasma with the addition of factor XIII concentrate at 2 IU ml$^{-1}$ (red curve) compared with a normal control plasma (black curve). After the measurement of the plasma viscosity (light blue area), the coagulation is triggered with PT reagents at time 0 s. Factor XIII deficiency does not affect the PT (all three times are in the normal range), but the clot strength is significantly low. After the addition of factor XIII concentrate, the final clot strength is restored to the normal range. (c) Differential mass adsorption (green area) onto surfaces functionalized with factor VIII antibodies, factor IX antibodies and quenched dithiobis(1-succinimidyl undecanoate) (qDSU, quenched with ethanolamine). Reciprocal of the sensor oscillation frequency signal-to-noise ratio (SNR$^{-1}$, pink area) during the stable clot phase (6 minutes after coagulation has been triggered). Both mass adsorption and SNR$^{-1}$ have been calculated from the sensor oscillation frequency signal (inset plot). After the measurement of the factor IX deficient plasma viscosity, the coagulation is triggered at time 0 min using aPTT reagents. As mentioned in part (c) brown curve, the aPTT is prolonged, indicating an intrinsic pathway's factor deficiency. The specific factor deficiency is then diagnosed through a differential measurement between the mass adsorption on anti-FVIII and anti-FIX surfaces (FVIII-FIX). The deficiency is finally confirmed by the increased SNR$^{-1}$ on anti-FVIII surfaces compared to anti-FIX surfaces.

regulations may lead to excessive clot formation and the creation of a thrombus (thrombosis). Fibrinolysis is an important part of the anticoagulation process that in conjunction with anticoagulant proteins leads to clot dissolution. An impaired function of the fibrinolytic system increases the risk of thrombosis.[43] Unfortunately, there is still a need for a robust global coagulation assay that can assess the fibrinolytic state.[2]

One approach that has been recently studied[9,10,44] is thromboelastography (TEG), where the clot strength is measured during clot formation and lysis. However, TEG does not provide absolute values (critical standardization) and does not allow to retain PT and aPTT information. Here we propose the use of microresonators to monitor clot formation triggered by PT reagents (tissue factor) and the simultaneous tissue plasminogen activator (tPA) naturally induced fibrinolysis (Fig. 5a). When plasminogen is activated to its active form called plasmin, it cleaves the fibrin network leading to the dissolution of the clot. The parameters that were extracted from these tests are: PT, starting clot strength (given by $C + B$, Fig. 5a), 50% lysis time (given by the time required to reach

 

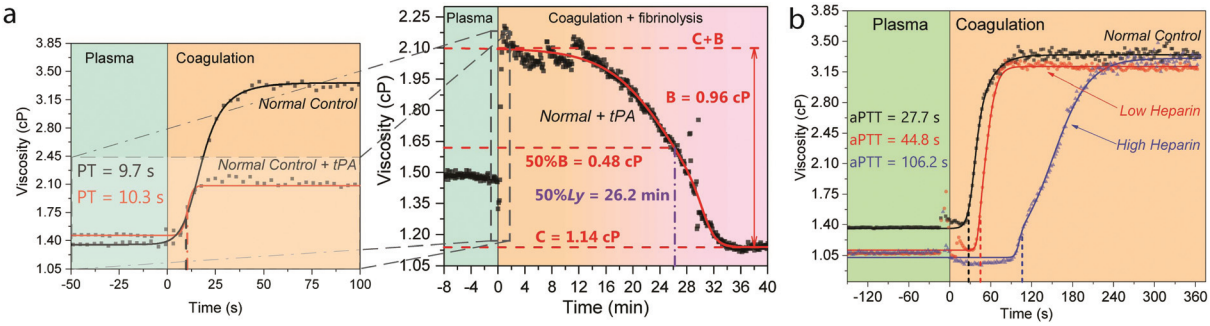


**Fig. 5** (a) Clot strength developing over time for tissue plasminogen activator (tPA) assisted fibrinolysis. Normal control plasma was mixed with a 350 ng ml$^{-1}$ tPA solution. After the measurement of the plasma viscosity, the coagulation is triggered at time 0 s with PT reagents. As soon as the coagulation is triggered, the clot strength increases, but at the same time the activity of tPA starts to lyse the fibrin network. After about 32 minutes, the clot is completely dissolved and the final strength is lower than the starting plasma viscosity. This difference is due to the fibrin breakage into soft fibrin particles that have no viscosity. Some of the parameters that can be extracted are PT (see zoom plot), starting clot strength (*C* + *B*), final dissolved clot strength (*C*), and time (50% Ly) required to reach half-clot strength (50% *B*). (b) Effects of heparin on the clot strength development during an aPTT test. After the measurement of the plasma viscosity, the coagulation is triggered at time 0 s with aPTT reagents. Higher concentrations of heparin cause more prolonged aPTT but the final clot strength is always in the normal range.

half the clot strength, Fig. 5a), and the final dissolved clot strength (parameter *C*, Fig. 5a). After triggering the coagulation, the clot strength was not stable due to simultaneous plasmin activity. The final dissolved clot strength was lower than the initial plasma viscosity. This is caused by the material breakage (plasmin activity) into soft fibrin particles that have no viscosity. Note that all the clot strengths are given in centipoise, which is an absolute unit for viscosity. Thrombosis treatment is often carried out with the use of heparin. Heparin is an antithrombotic drug that binds and activates the coagulation inhibitor antithrombin. We studied the effects of heparin on the development of the clot strength during coagulation by testing different (low and high) heparin concentrations added to normal control plasma samples (Fig. 5b). Notably, heparin can delay clot formation (prolonged aPTT), but once the coagulation starts the final clot strength was in the normal range.

## Conclusions

The diagnosis of blood coagulation disorders often requires multiple tests. If a patient has bleeding symptoms, the most common assays are the prothrombin time (PT) and the activated partial thromboplastin time (aPTT). They are used as starting points for the diagnosis of a particular factor deficiency or inhibitor. When coagulation times are prolonged, a factor deficiency of the extrinsic (PT) or intrinsic (aPTT) or common (both PT and aPTT) coagulation pathway (see Fig. 1a) is normally expected.[2] To confirm the diagnosis, other tests are required, such as immunoassays that can detect the presence of a specific factor or inhibitor. Furthermore, both coagulation time assays and antigen assays do not evaluate the mechanical properties of the blood clot, such as plasma viscosity and clot strength. In recent years, global hemostasis assays have gained attention. They provide the real-time information about the development of the blood clot viscoelastic properties. However, these assays represent a separate group of analytical tools in comparison with simple coagulation time assays, they present issues with standardization,[5] and do not provide coagulation times such as PT and aPTT. We have demonstrated that it is possible to combine the essential PT and aPTT assays with global hemostasis assays in one single test. We have applied suspended microresonators (in a 4 μl microfluidic chamber) to greatly reduce the amount of blood needed (20 μl, fingerprick), and to achieve the required temporal and clot strength sensitivity. Our novel approach proves to be suitable for a wide range of blood related disorders. First of all, it is possible to study the initial status (plasma viscosity) and the clot strength changes during clot initiation, formation, and lysis (see Fig. 1c). Secondly, we successfully diagnosed a specific factor deficiency such as haemophilia or factor XIII deficiency. Factor XIII deficiency would present normal aPTT and PT, but it is a severe bleeding disorder. It is a fundamental factor that cross-links the fibrin network, therefore increasing the clot strength and stabilizing the hemostatic plug. Thirdly, we have studied tissue plasminogen activator (tPA) assisted fibrinolysis. Fibrinolysis is a fundamental part of the anticoagulation cascade. It prevents abnormal and uncontrolled growth of the blood clot that would eventually lead to thrombosis. Finally, we tested the effects of anticoagulant treatments, such as heparin, on the coagulation times and on the clot strength development. Note that a prolonged aPTT or PT is not uniquely an indication of a factor deficiency. The factor concentration might in fact be normal, but an inhibitor could be present. Almost no studies have provided evidence-based laboratory medicine on how to proceed with inhibitor screening studies.[2] For instance, in haemophilia factor replacement treatment, one of the complications is the development of autoantibodies (inhibitors) that interfere with the coagulation factor. In order to detect this inhibition, we showed that a simple approach could be the addition of the specific factor to

the deficient plasma *in vitro*. If the coagulation time and/or the clot strength is restored, an inhibition can be excluded (see Fig. 4c). Another approach is the modification of the sensor surfaces to immobilise factor specific antibodies. The factor deficiency can then be diagnosed through differential mass adsorption that quantifies the specific antigen–antibody interaction (immunoassay). We believe that the presented technology will improve coagulation testing in a broad range of blood related disorders, from specific factor deficiency to global coagulation parameters, such as initial plasma viscosity and clot strength, to the assessment of fibrinolysis. The small volumes required, along with quick and reliable measurements make this approach suitable for the clinical coagulation testing and diagnostics. Also, the small sensor size (μm size range) provides the possibility to miniaturise this device for point-of-care testing.

## Conflicts of interest

There are no conflicts to declare.

## Acknowledgements

We thank M.D. Nicoló Marchesini at the University of Verona, Department of Medicine for expert advice. We thank Robert Bristow-Johnson for his help with phase spectra measurements. The work was supported by Science Foundation Ireland under the IvP scheme SFI/09IN/1B2623 and SFI/15/IA/3023 and the CSET scheme SFI/10/CSET/B1821.

## References

1 K. G. Mann, *Chest*, 2003, **124**, 4S–10S.
2 R. A. McPherson and M. R. Pincus, *Henry's clinical diagnosis and management by laboratory methods*, Elsevier Health Sciences, 2016.
3 H. Hartert, *Klin. Wochenschr.*, 1948, **26**, 577–583.
4 M. T. Ganter and C. K. Hofer, *Anesth. Analg.*, 2008, **106**, 1366–1375.
5 A. Sankarankutty, B. Nascimento, L. T. da Luz and S. Rizoli, *World J. Emerg. Surg.*, 2012, **7**, S3.
6 L. T. da Luz, B. Nascimento and S. Rizoli, *Scand. J. Trauma Resusc. Emerg. Med.*, 2013, **21**, 29.
7 E. N. Lipets and F. I. Ataullakhanov, *Thromb. J.*, 2015, **13**, 4.
8 N. K. Thalji, L. Ivanciu, R. Davidson, P. A. Gimotty, S. Krishnaswamy and R. M. Camire, *Nat. Med.*, 2016, **22**, 924–932.
9 G. F. Genét, S. R. Ostrowski, A. M. Sørensen and P. I. Johansson, *Clin. Appl. Thromb./Hemostasis*, 2012, **18**, 638–644.
10 J. L. Kashuk, E. E. Moore, M. Sawyer, M. Wohlauer, M. Pezold, C. Barnett, W. L. Biffl, C. C. Burlew, J. L. Johnson and A. Sauaia, *Ann. Surg.*, 2010, **252**, 434–444.
11 T. Matsumoto, K. Nogami and M. Shima, *Thromb. Haemostasis*, 2013, **110**, 761–768.
12 A. Antovic, *Semin. Thromb. Hemostasis*, 2010, **36**, 772–779.
13 R. S. Lakshmanan, V. Efremov, J. S. O'Donnell and A. J. Killard, *Anal. Bioanal. Chem.*, 2016, **408**, 6581–6588.
14 A. Sellborn, M. Andersson, C. Fant, C. Gretzer and H. Elwing, *Colloids Surf. B*, 2003, **27**, 295–301.
15 T. P. Vikinge, K. M. Hansson, J. Benesch, K. Johansen, M. Ranby, T. L. Lindahl, B. Liedberg and P. Tengvall, *J. Biomed. Opt.*, 2000, **5**, 51–55.
16 K. Hansson, T. P. Vikinge, M. Rånby, P. Tengvall, I. Lundström, K. Johansen and T. Lindahl, *Biosens. Bioelectron.*, 1999, **14**, 671–682.
17 F. Padovani, J. Duffy and M. Hegner, *Anal. Chem.*, 2017, **89**, 751–758.
18 C. A. Van Eysden and J. E. Sader, *J. Appl. Phys.*, 2007, **101**, 044908.
19 H. Etayash, A. McGee, K. Kaur and T. Thundat, *Nanoscale*, 2016, **8**, 15137–15141.
20 P. M. Kosaka, V. Pini, J. Ruz, R. Da Silva, M. González, D. Ramos, M. Calleja and J. Tamayo, *Nat. Nanotechnol.*, 2014, **9**, 1047–1053.
21 N. Maloney, G. Lukacs, J. Jensen and M. Hegner, *Nanoscale*, 2014, **6**, 8242–8249.
22 S. Wu, Z. Zhang, X. Zhou, H. Liu, C. Xue, G. Zhao, Y. Cao, Q. Zhang and X. Wu, *Nanoscale*, 2017, DOI: 10.1039/c7nr03688d.
23 S. Federici, G. Oliviero, D. Maiolo, L. E. Depero, I. Colombo and P. Bergese, *J. Colloid Interface Sci.*, 2012, **375**, 1–11.
24 S. Federici, G. Oliviero, K. Hamad-Schifferli and P. Bergese, *Nanoscale*, 2010, **2**, 2570–2574.
25 M. K. Ghatkesar, E. Rakhmatullina, H.-P. Lang, C. Gerber, M. Hegner and T. Braun, *Sens. Actuators, B*, 2008, **135**, 133–138.
26 E. Lemaire, M. Heinisch, B. Caillard, B. Jakoby and I. Dufour, *Meas. Sci. Technol.*, 2013, **24**, 084005.
27 B. A. Bircher, L. Duempelmann, K. Renggli, H. P. Lang, C. Gerber, N. Bruns and T. Braun, *Anal. Chem.*, 2013, **85**, 8676–8683.
28 P. Roach, D. Farrar and C. C. Perry, *J. Am. Chem. Soc.*, 2005, **127**, 8168–8173.
29 T. Braun, V. Barwich, M. K. Ghatkesar, A. H. Bredekamp, C. Gerber, M. Hegner and H. P. Lang, *Phys. Rev. E: Stat. Phys., Plasmas, Fluids, Relat. Interdiscip. Top.*, 2005, **72**, 031907.
30 R. Biggs, *Human Blood Coagulation, Haemostasis and Thrombosis*, Blackwell Scientific Publications, 2nd edn, 1976.
31 M. Walther, P. M. Fleming, F. Padovani and M. Hegner, *EPJ Tech. Instrum.*, 2015, **2**, 1–24.
32 Y. Arntz, J. D. Seelig, H. Lang, J. Zhang, P. Hunziker, J. Ramseyer, E. Meyer, M. Hegner and C. Gerber, *Nanotechnology*, 2002, **14**, 86.
33 M. H. Jazayeri, H. Amani, A. A. Pourfatollah, H. Pazoki-Toroudi and B. Sedighimoghaddam, *Sens. Biosensing Res.*, 2016, **9**, 17–22.

 

34 P. Wagner, M. Hegner, P. Kernen, F. Zaugg and G. Semenza, *Biophys. J.*, 1996, **70**, 2052–2066.
35 O. Cakmak, C. Elbuken, E. Ermek, A. Mostafazadeh, I. Baris, B. E. Alaca, I. H. Kavakli and H. Urey, *Methods*, 2013, **63**, 225–232.
36 M. Hanss and F. Biot, *Ann. N. Y. Acad. Sci.*, 2001, **936**, 89–90.
37 M. Lak, M. Keihani, F. Elahi, F. Peyvandi and P. Mannucci, *Br. J. Haematol.*, 1999, **107**, 204–206.
38 E. Dupuy, C. Soria, P. Molho, J.-M. Zini, S. Rosenstingl, C. Laurian, P. Bruneval and G. Tobelem, *Thromb. Res.*, 2001, **102**, 211–219.
39 V. Blanchette, N. Key, L. Ljung, M. Manco-Johnson, H. Berg and A. Srivastava, *J. Thromb. Haemostasis*, 2014, **12**, 1935–1939.
40 A. Pavlova and J. Oldenburg, *Semin. Thromb. Hemostasis*, 2013, **39**, 702–710.
41 L. Hsieh and D. Nugent, *Haemophilia*, 2008, **14**, 1190–1200.
42 E. Dorey, *Nat. Biotechnol.*, 2014, **32**, 210–210.
43 M. E. Meltzer, C. J. Doggen, P. G. de Groot, F. R. Rosendaal and T. Lisman, *Semin. Thromb. Hemostasis*, 2009, **35**, 468–477.
44 A. Kupesiz, M. Rajpurkar, I. Warrier, W. Hollon, O. Tosun, J. Lusher and M. Chitlur, *Blood Coagulation Fibrinolysis*, 2010, **21**, 320–324.